Correlations of Prompt and Afterglow Emission in *Swift* Long and Short Gamma Ray Bursts

N. Gehrels[1], S.D. Barthelmy[1], D.N. Burrows[2], J.K. Cannizzo[1,3], G. Chincarini[4,5], E. Fenimore[6], C. Kouveliotou[7], P. O'Brien[8], D.M. Palmer[6], J. Racusin[2], P.W.A. Roming[2], T. Sakamoto[1,3], J. Tueller[1], R. Wijers[9], B. Zhang[10]

[1] NASA-Goddard Space Flight Center, Greenbelt, MD 20771, USA, neil.gehrels@nasa.gov
[2] Department of Astronomy & Astrophysics, Pennsylvania State University, State College, PA 16802 USA
[3] Oak Ridge Associated Universities, P.O. Box 117, Oak Ridge, TN, 37831-0117, USA
[4] INAF-Osservatorio Astronomico di Brera, 1-23807 Merate, Italy
[5] Universita degli studi di Milano Bicocca, 1-20126, Milano, Italy
[6] Los Alamos National Laboratory, P.O. Box 1663, Los Alamos, NM, 87545, USA
[7] NASA-Marshall Space Flight Center, NSSTC, VP-62, 320 Sparkman Drive, Huntsville, AL 35805, USA
[8] Department of Physics & Astronomy, University of Leicester, Leicester, LE1 7RH, UK
[9] Faculty of Science, Astronomical Institute `Anton Pannekoek', University of Amsterdam, Kruislaan 403, 1098 SJ Amsterdam, The Netherlands
[10] Department of Physics and Astronomy, University of Nevada Las Vegas, Las Vegas, NV 89154, USA

ABSTRACT

Correlation studies of prompt and afterglow emissions from gamma-ray bursts (GRBs) between different spectral bands has been difficult to do in the past because few bursts had comprehensive and intercomparable afterglow measurements. In this paper we present a large and uniform data set for correlation analysis based on bursts detected by the *Swift* mission. For the first time, short and long bursts can be analyzed and compared. It is found for both classes that the optical, X-ray and gamma-ray emissions are linearly correlated, but with a large spread about the correlation line; stronger bursts tend to have brighter afterglows, and bursts with brighter X-ray afterglow tend to have brighter optical afterglow. Short bursts are, on average, weaker in both prompt and afterglow emissions. No short bursts are seen with extremely low optical to X-ray ratio as occurs for 'dark' long bursts. Although statistics are still poor for short bursts, there is no evidence yet for a subgroup of short bursts with high extinction as there is for long bursts. Long bursts are detected in the dark category at the same fraction as for pre-*Swift* bursts. Interesting cases are discovered of long bursts that are detected in the optical, and yet have low enough optical to X-ray ratio to be classified as dark. For the prompt emission, short and long bursts have different average tracks on flux *vs* fluence plots. In *Swift*, GRB detections tend to be fluence limited for short bursts and flux limited for long events.

1. INTRODUCTION

One of the longest enduring Gamma Ray Burst (GRB) classification schemes is based on their distributions in duration and spectral hardness. Both quantities seem to cluster into two separate classes with the longer events (those above ~2 s; Kouveliotou et al. 1993) being predominantly softer while the shorter ones are harder. The mechanism for the origin of the GRB explosions (the central engine) appears to be quite different for the two types (van Paradijs, Kouveliotou & Wijers 2000, and references therein). Long bursts are ascribed to the core collapse to a black hole of a massive, young, rapidly rotating star in the 'collapsar' model (Woosley 1993; MacFadyen & Woosley 1999; Woosley & Bloom 2007) which is supported by observations such as the coincidence of SNe with well-observed nearby GRBs (Galama et al. 1998; Bloom et al. 1999; Staneck et al. 2003; Hjorth et al. 2003). The prevalent model for short bursts suggests they are caused by the coalescence of a binary pair of compact old stars (Lattimer & Schramm 1974; Paczynski 1986; Eichler et al. 1989; Mochjkovitch et al. 1993) which is supported by recent observations of progenitor sites with low star formation activity (Gehrels et al. 2005; Bloom et al. 2006; Fox et al. 2005; Villasenor et al. 2005, Hjorth et al. 2005; Barthelmy et al. 2005; Berger et al. 2005). In both scenarios, a highly-relativistic collimated outflow of particles and radiation (jet) occurs producing prompt gamma-ray emission from shock accelerated electrons, which evolves into a long-lasting afterglow from shock interactions with the circumburst medium (e.g., Mészáros & Rees 1997). For short bursts there are also models for the afterglow in which a radioactive wind causes emission in the first day or so (Li & Paczynski 1998).

Correlation studies of prompt and afterglow emission are crucial for understanding their production mechanisms and environmental effects. For example, Jakobsson et al. (2004) developed a criterion for determining which GRBs are 'dark' bursts, by comparing the relative intensity of their X-ray and optical afterglows to find what fraction of bursts have high column densities. Roming et al. (2006) and Fynbo et al. (2007) expanded that work to include (long) bursts from the *Swift* satellite. A more detailed work on dark bursts using a broad-band spectral analysis is given by Rol et al. (2005, 2007). Zhang et al. (2007) have a study comparing radiative efficiencies for short and long bursts as derived from a correlation analysis. Using *Swift* short bursts, Berger (2007) compared their X-ray afterglow to their gamma-ray prompt emission, and found that 20% have anomalously low X-ray to gamma ray ratios indicating very low density burst sites, possibly in globular clusters, for that subpopulation. Thus, correlation studies are useful for determining the properties of long and short bursts, and particularly the properties of the circuburst environment. To date there has not been an comprehensive analysis of the correlations for both classes.

In this paper we perform correlation studies using the extensive data set from *Swift*. Sections 2 and 3 cover observations and results, respectively, while in Section 4, we discuss the implications of the results and in Section 5 the conclusions and future prospects.

2. OBSERVATIONS

2.1 Swift Studies

The *Swift* mission (Gehrels et al. 2004) has so far provided *uniform observations of prompt and afterglow emission* for hundreds of GRBs. This sample is an order of magnitude larger than the one previously available with e.g., the BeppoSAX satellite (see, web site by J. Grenier: http://www.mpe.mpg.de/~jcg /grbgen.html). Further, *Swift* X-ray observations covering time-scales from 1 minute to several days after the burst are provided for the first time for almost every GRB. After three years of operations, our data set has now reached a critical size where statistically meaningful correlations can be studied.

We present here three correlation studies: 1) X-ray *vs* optical afterglow, 2) gamma-ray prompt *vs* X-ray afterglow, and 3) prompt gamma-ray peak flux *vs* fluence. All the data used in this study are listed in Tables 1-4 except that gamma-ray data are listed only for those busts with, at least, an X-ray afterglow. The full list of fluences and fluxes for the 193 bursts used for study #3 are directly from the Sakamoto et al. (2007) tables. We include all *Swift* bursts from January 2005 through July 2007 for studies 1 and 2 and through February 2007 for study 3.

For the X-ray *vs* optical afterglow study, we use the methods developed by Jakobsson et al. (2004) in their comparison of X-ray and optical afterglow fluxes for pre-*Swift* bursts. In order to compare to the Jakobsson et al. results, we use the same definition of quantities: the X-ray flux at 3 keV, the optical flux in the R-band, and sampling time at 11 hours after the burst. The *Swift* X-ray lightcurves have been found to typically have complex shapes (Nousek et al. 2005; Zhang et al. 2005) often including a poorly understood 'flat phase'; the use of flux at 11 hours in most cases avoids sampling during the flat phase and gives a measure of the true burst afterglow.

2.2 X-ray Fluxes

The X-ray fluxes are from measurements of the *Swift* X-Ray Telescope (XRT; Burrows et al. 2005). Our primary data product for the XRT flux is the integral flux between 0.3 and 10 keV corrected for absorption at low energies (unabsorbed flux). This is converted to the differential flux at 3 keV using the measured spectral index. The integral fluxes, photon spectral indices and differential fluxes are listed in Tables 1-3. A 10% systematic uncertainty was added in quadrature to the measured error to account for uncertainties in the shape and variability of the lightcurves.

Details of the integtral flux calculation are as follows. Level 1 data products were downloaded from the NASA/GSFC *Swift* Data Center (SDC) and processed using XRTDAS software (v2.0.1). The *xrtpipeline* task was used to generate level 2

cleaned event files. Only events with Windowed Timing (WT) mode grades 0-2 and Photon Counting (PC) mode grades 0-12 and energies between 0.3-10.0 keV were used in subsequent temporal and spectral analysis.

The XRT light curves were created by extracting the counts in a circular region around the GRB afterglow with a variable source radius designed to optimize the S/N depending on the count rate. They were background subtracted, pile-up corrected were applicable, exposure map corrected, and corrected for the fraction of the PSF excluded by the extraction region. The number of counts per bin is variable and dependent on the count rate. Time intervals of significant flaring were removed from the light curves and they were fit to power-laws, broken power-laws, and multiply broken power-law. Using these temporal fits, we interpolated the count rate at 11 hours.

Spectra for the power-law segments of the light curves were extracted individually to limit contamination by potential spectral variability. The segment used for the counts to flux conversion was that which spanned 11 hours. The spectra were created by extracting the counts in a 20 pixel radius extraction region and a 40 pixel radius background region. The Ancillary Response Files were made using the *xrtmkarf* task and grouped with 20 counts per bin using the *grppha* task. The spectra were fit in XSPEC to absorbed power-laws and used to measure the 0.3-10 keV flux and count rate which was applied to the interpolated count rate to convert into flux units.

2.3 Optical and Gamma Ray Fluxes

The optical fluxes are from measurements by ground-based telescopes and from the *Swift* UV Optical Telescope (UVOT; Roming et al. 2005). An extensive literature search was done to find the best optical data for each burst. Bursts were included in the study if measurements were available within a factor of 2 of 11 hours (i.e., at >5.5 hours or <22 hours). The value at 11 hours was estimated by interpolations and extrapolations when measurements were not available exactly at 11 hours. The one exception to the factor-2 criterion was GRB 070508 with measurements to only 4 hours, which was included because it appears to be an interesting dark burst candidate. A few bursts are listed with optical flux upper limits at the bottom of Table 2. This is not an exhaustive list of optical limits, but only those with low optical to X-ray ratio limits. A 10% systematic uncertainty was added in quadrature to the measured error to account for uncertainties in the shape and variability of the lightcurves.

The gamma-ray fluences and peak fluxes are in the 15-150 keV band and are from the *Swift* Burst Alert Telescope (BAT; Barthelmy et al. 2005) as compiled in the BAT GRB catalog (Sakamoto et al. 2007). For the gamma-ray flux needed in study #3, we use 1 s binning as quoted by Sakamoto et al. (2007).

2.4 Correlation Analysis

For each study, we have performed fits to the two-parameter correlation data using the Spearman rank test (Spearman 1904) and derived the correlation coefficient, r, to determine the degree and significance of the correlation. Upper limits were not included in the fits. In the Spearman rank test, the probability of a null correlation, P_{null}, is given by

$$P_{null} = \mathrm{erfc}\ (r * \mathrm{sqrt}(N/2))$$

where N is the number of data points. The significance of the correlation is $P_{cor} = 1 - P_{null}$. The fraction of the observed spread of the data that can be explained by the correlation is given by r^2. The fit parameters and correlation r values are listed in Table 4.

3. RESULTS

3.1 X-ray and Optical Afterglow Correlations

Figure 1 shows the *Swift* X-ray afterglow average flux at 3 keV as a function of the R-band optical flux, both converted to μJy at 11 hours after the burst, for short and long bursts. The pre-*Swift* data points are taken from Jakobsson et al. (2004) and are shown as filled gray points. Also shown is the solid line of constant X-ray to optical spectral index that they propose separates the true 'dark' bursts from the rest. As listed in Table 4, the Spearman rank test for the two GRB populations in Figure 1 gives a null probability of 0.13 or an 87% correlation probability between the optical and X-ray flux of the long GRBs, and only 57% for the short population.

The long *Swift* GRBs fall in the same general region of the plot as the pre-*Swift* ones. As with the pre-*Swift* bursts, several *Swift* long bursts (detections and upper limits) also fall below the Jakobsson et al. dark line. The brightest short GRBs fall within the midst of the long GRB points, but in the region toward lower fluxes. The dimmest short GRBs extend significantly below the long burst population. To date there are no short bursts that fall below the dark burst line; those with low optical fluxes or upper limits tend to also have weak X-ray fluxes that place them above the line.

3.2 Gamma Ray Prompt and X-ray Afterglow Correlations

We show in Figure 2 the average X-ray afterglow flux *vs* the gamma-ray fluence of the prompt emission for long and short *Swift* GRBs. We find a highly significant correlation (99.9996% probability) for the long GRBs, albeit with a wide spread in the data. The correlation of the short bursts is less significant (95%

probability) mostly due to the smaller number of points. There is an overlap between the brightest short bursts and the faintest long GRBs. The weakest short bursts are fainter than the weakest long bursts.

3.3 Prompt Gamma Ray Fluence and Peak Flux Correlations

Figure 3 shows the prompt emission fluence as a function of peak flux for GRBs detected by BAT. We see a linear correlation for both short and long bursts with a significant spread in the correlation. The correlation probability is virtually 100% (null probability = 2×10^{-20}) for long bursts and 96% for short bursts. The best fit lines are distinctly different for short and long bursts, with the long burst having a higher fluence on average for a given flux level than short bursts as expected from duration alone.

4. DISCUSSION

4.1 Correlations & Short/Long Distributions

We show in this paper that correlations exist between prompt and afterglow fluxes of GRBs and between different wavelength bands in the afterglow. The highest significance correlation is between the prompt emission gamma-ray fluence and the X-ray afterglow flux at a significance level of 99.9996% for long bursts and 95% for short bursts. The correlation between the optical afterglow and X-ray afterglow fluxes is less significant at 87% significance for long bursts and only 57% for short bursts. It is important to note that there is a wide spread in the data for all of the correlations. The correlations are real and significant, but the fraction of the observed variations due to the correlations between the above parameters accounts for only a portion of the data spread. The correlation can only be used to predict a flux level to within approximately an order magnitude. The fraction of the variation due to the correlations is given by the square of the correlation parameter, r, which, as shown in Table 4, varies from a few percent to 50%. The rest of the data spread is due to other factors such as correlations with additional unknown parameters. An example of an additional parameter is extinction in the optical afterglow.

Short bursts are weaker on average than long bursts in afterglow fluxes. There is overlap with the dimmer long bursts, but the short bursts extend to lower intensities than seen for long bursts. The average X-ray flux at 3 keV at 11 hours for the short bursts is $\langle F_x(\text{short}) \rangle = 9.3 \times 10^{-3}$ μJy, which is more than an order of magnitude less than the average for long bursts of $\langle F_x(\text{long}) \rangle = 1.3 \times 10^{-1}$ μJy.

The correlation power-law fits in Table 4 show some differences between long and short bursts in all 3 studies. However, for the first two studies (optical *vs* X-ray afterglow and gamma-ray prompt *vs* X-ray afterglow) the differences between the fits

are statistically marginal of less than 3σ significance. From the analysis of Zhang et al. (2007), the implication of this result is that the radiative efficiency is similar for long and short GRBs. For the prompt emission fluence *vs* flux study, the differences are highly statistically significant as expected from the very fact that short and long bursts have different durations as discussed below.

4.2 Dark GRBs

Another comparison of short and long GRBs relates to dark bursts. Jakobsson et al. (2004) used the simple criterion to define dark bursts as those with extremely low optical to X-ray afterglow ratio, falling below the line of optical to X-ray spectral index, β_{OX}, equal to 0.5. It may seem counterintuitive that there can be dark bursts with optical detections and bursts not detected in the optical that are not 'dark', but the important criterion is how optically faint the burst is relative to its X-ray flux. For the pre-*Swift* sample there were 5 bursts with upper limits below the dark-burst line compared to 24 bursts with actual measurements (not upper limits) above the line, giving a fraction of ~17% in the dark category. For *Swift* there are 4 bursts with upper limits (GRB 050713B, 061222A, 070621, & 070704) and 3 cases with measurements (GRB 060210, 070419B & 070508) below the line compared with 34 longs bursts above the line for a fraction of ~17% in the dark category, exactly the same as the pre-*Swift* sample. The conclusion is that *Swift* is sampling the same source environments as previously instruments.

The discovery of 3 cases of dark bursts with optical detections is particularly interesting. On possible concern with this finding is that *Swift* X-ray afterglows are contaminated in many bursts by emission components not from the external shocks, e.g. X-ray flares. In such instances, the Jakobsson et al. (2004) approach to define dark bursts is no longer relevant since it assumes that the X-ray and optical emission is from the same emission component, but separated by a cooling break. However, the X-ray lightcurves for the *Swift* dark bursts are smooth around 11 hours with no significant contamination from other components. These are real "dark" bursts from both an observational and physics perspective.

For the first time we can search for dark short bursts. No short bursts are seen that fall below the dark-burst line. It is hard to find dark GRBs using this criterion since X-ray afterglow fluxes are also low for the short bursts. However, there are some short bursts with bright X-ray afterglow, and, to date, none of those is seen to be highly deficient in optical afterglow. Statistics are still small with only 5 optical detections, but if the observed trend continues we will be able to conclude that short bursts do not occur in regions with extremely high extinction as occurs for some long bursts.

4.3 Prompt Fluence and Flux Comparisons

The comparison of fluences and peak fluxes in the prompt emission as shown in Figure 3 is a different kind of study than in the other two above. In this case, the strong observed correlation and high degree of separation of short and long bursts is expected; brighter bursts with higher peak fluxes naturally have higher fluences and short bursts tend to have lower fluence for a given flux by the very fact of their short duration. Within the short and long classes, the spread in fluence that is seen for a given peak flux is due to the diversity of durations and spectral indices. Bursts with longer duration and hard spectra have higher fluences for the same peak flux.

It is interesting to note in Figure 3 that the short bursts tend to be fluence limited in the BAT, while long bursts tend to be peak flux limited. This is due to the way BAT operates. A valid GRB trigger requires a statistically significant excess in both the rate and image domains (Fenimore et al. 2004). The ability to form an image depends on the number of photons collected on various trigger timescales, which is related to the burst fluence. Even for relatively high peak-fluxes, short bursts can have low fluences values and be limited in the number of photons available for the image trigger. On the other hand, long bursts tend to have higher fluences for a given peak-flux and become rate limited before the image limit is reached. BAT also has a pure-image mode for triggering where very long duration GRBs and other transients are found by comparing sky images instead of having a rate trigger. The lowest long-burst point in Figure 3 at a peak flux of ~0.1 was such an image-mode trigger for the very long (T_{90} = 35 min) and weak GRB 060218. A caveat on the above discussion is that the BAT trigger algorithm is complex with ~500 different trigger criteria evaluated. There are many different thresholds and limits coming into play for short and long burst triggering, with some mix of flux and fluence limits for both types.

This study was based on a 1 s binning for the gamma-ray fluxes. We have also investigated the effect of using a smaller bin size of 64 ms. Smaller bins pick out larger peak flux values when there is short time structure or when the burst has a duration shorter than the bin size. The effect of the smaller bin size is to shift the short bursts to the right (higher peak flux) relative to the long bursts by about a factor of 5. The larger bin size that we used for the figure in this paper has better statistics and is more reliable for long bursts. In either case the short bursts tend toward lower fluences than long bursts.

5. FUTURE PROSPECTS

The combined prompt and afterglow data set for *Swift* GRBs is the largest available to date. We have chosen a criterion on the afterglow measurements for inclusion in this study of being a solid measurement 11 hours after the burst. Even with this stringent definition, there are more than 100 long bursts with X-ray afterglow data. The optical detections at 11 hours are less numerous with about 40 good measurements, but still enough statistics for conclusions to be reached.

The short burst correlations studies are possible now and key results are beginning to emerge. The *Swift* data base is growing quickly with time. In its expected lifetime of ~10 years, the mission should provide a sample of >40 short and >400 long GRBs with good afterglow and prompt observations. The hints of a diverse population of short bursts in the current correlation plots and significant differences compared to long bursts predict an interesting future for this work.

Acknowledgements:

The authors thank the following people for useful discussions: J. Fynbo, P. Jakobsson, A. Loeb, M. Nysewander, and E. Rol.

REFERENCES

Antonelli, L. A., et al. 2006, A&A, 456, 509

Barthelmy, S. D., et al. 2005, Space Sci Rev, 120, 143.

Barthelmy, S. D., et al. 2005, Nature, 438, 994

Schmidt, B., & Bayliss, D. 2006, GCN 4880

Berger, E., et al. 2005, Nature, 438, 988.

Berger, E. et al. 2006, GCN 5697

Berger, E., & Soderberg, A. M. 2005, GCN 4419

Berger, E. 2007 ApJ, in press (astro-ph 0702694)

Berger, E., et al. 2006, ApJ, in press (astro-ph 0611128)

Bikmaev, I., et al. 2005, GCN 3797

Bloom, J. S., et al. 1999, Nature, 401, 453.

Bloom, J.S., et al. 2006, ApJ, 638, 354.

Burrows, D.N., et al. 2005, Space Sci Rev, 120, 165.

Butler, N. R., et al. 2006, ApJ, 652, 1390

Cenko, S. B., Fox, D. B., & Price, P. A. 2006, GCN 5912

Cenko, S. B., et al. 2006, ApJ, 652, 490

Chen, H.-W., et al. 2007, ApJ, 663, 420

Cobb, B. E., & Bailyn, C. D. 2005, GCN, 3104

Curran, P. A., et al. 2007a, MNRAS, 381, L65

Curran, P. A., et al. 2007b, A\&A, 467, 1049

Dado, S., Dar, A., \& De Rujula, A. 2007, astro-ph/0706.0880v1

Dai, X., et al. 2007, ApJ, 658, 509

D'Avanzo, P., et al. 2006, GCN 5884

Della Valle, M., et al. 2006, ApJ, 642, L103

Durig, D. T., \& Price, A. 2005, GCN, 4023, http://gcn.gsfc.nasa.gov/gcn3/4023.gcn3

Efimov, Yu. et al. 2006, GCN 5986

Eichler, D., Livio, M., Piran, T., & Schramm, D. N. 1989, Nature, 340, 126.

Fenimore, E., et al. 2004, AIP, 727, 667.

Fox, D.B., et al. 2005, Nature, 437, 845.

Fynbo, J.P.U., et al. 2007 astro-ph 0703458.

Fynbo, J. P. U., et al. 2006, Nature, 444, 1047

Galama, T. J., et al. 1998, Nature, 395, 670.

Garnavich, P., & Karska, A. 2006, 5253, http://gcn.gsfc.nasa.gov/gcn3/5253.gcn3

Gehrels, N., et al. 2004, ApJ, 611, 1005.

Gehrels, N., et al. 2005, Nature, 437, 859.

George, K., Banerjee, D. P. K., Chandrasekhar, T., & Ashok, N. M. 2006, ApJ, 640, L13

Ghirlanda, G., Nava, L., Ghisellini, G., & Firmani, C. 2007, A&A, 466, 127

Guidorzi, C., et al. 2007a, A&A, 463, 539

Hicken, M., & Garnavich, P. 2006, GCN, 5070, http://gcn.gsfc.nasa.gov/gcn3/5070.gcn3

Hjorth, J., et al. 2003, Nature, 423, 847.

Hjorth, J., et al. 2005, Nature, 437, 851.

Huang, K. Y., et al. 2007, ApJ, 654, L25

Jakobsson, P., et al. 2004, ApJ, 617, L21.

Kamble, A., Resmi, L., & Misra, K. 2007, ApJ, 664, L5

Kouveliotou, C., et al. 1993, ApJ, 413, L101.

Lattimer, J. M. & Schramm, D. N. 1974, ApJ, 192, L145.

Lee, W.H., & Ramirez-Ruiz, E. 2007, New J. Phys., 9, 17

Levan, A. J., et al. 2007, GCN 6630

Li, L.-X. & Paczynski, B. 1998, ApJ, 507, L59

MacFadyen, A. I. & Woosley, S. E. 1999, ApJ, 524, 262

Malesani, D., et al. 2007, GCN 6565

Malesani, D., et al. 2007, GCN 6674

Malesani, D., et al. 2007, A&A, 473, 77

Melandri, A., Rol, E., & Tanvir, N. 2007, GCN, 6602

Melandri, A., Tanvir, N., & Guidorzi, C. 2006, GCN, 5322,
http://gcn.gsfc.nasa.gov/gcn3/5322.gcn3

Mészáros, P. & Rees, M.J. 1997, ApJ, 476, 232.

Milne, P. A. 2006, GCN, 5127, http://gcn.gsfc.nasa.gov/gcn3/5127.gcn3

Misra, K., & Pandey, S. B. 2005, GCN 3396

Misra, K., et al. 2007, A&A, 464, 903

Mochkovitch, R., et al. 1993, Nature 361, 236.

Monfardini, A., et al. 2006, ApJ, 648, 1125

Mundell, C. G., et al. 2007, ApJ, 660, 489

Nakar, E., et al. 2007, Phys Reports, 442, 166.

Nousek, J.A., et al. 2006, ApJ, 642, 389.

Nysewander, M., et al. 2007, astro-ph/0608.3444v2

Oates, S. R., et al. 2006, MNRAS, 372, 327

Paczynski, B. 1986, ApJ, 308, L43.

Page, K. L., et al. 2007, ApJ, 663, 1125

Pandey, S. B., et al. 2006, A&A, 460, 415

Perley, D. A., et al. 2007, astro-ph/0703538v2

Price, P. A., et al. 2006, GCN 5077

Quimby, R., & Rykoff, E. S. 2006, GCN, 5377, http://gcn.gsfc.nasa.gov/gcn3/5377.gcn3

Rol, E., et al. 2005, ApJ, 624, 868

Rol, E., et al. 2007, ApJ, 669, 1098

Roming, P.W.A., et al. 2005, Space Sci Rev, 120, 95.

Roming, P.W.A., et al. 2006, ApJ, 652, 1416.

Rykoff, E. S., et al. 2006, ApJ, 638, L5

Sakamoto, T., et al. 2007, ApJ, submitted (astro-ph 0707.4626).

Sakamoto, T., et al. 2006, in "Gamma-Ray Bursts in the Swift Era", ed. S.S. Holt, N. Gehrels and J.A. Nousek (AIP: New York), p. 43

Schmidt, B., \& Mackie, G. 2007, GCN, 6325, http://gcn.gsfc.nasa.gov/gcn3/6325.gcn3

Sharapov, D. et al. 2007, GCN 3701

Shao, L., & Dai, Z. G. 2005, ApJ, 633, 1027

Soderberg, A. M., et al. 2006, ApJ, 650, 261

Soderberg, A. M., et al. 2007, ApJ, 661, 982

Sollerman, et al. 2007, A&A, 466, 839

Soyano, T., Mito, H., & Urata, Y. 2006, GCN, 5548,
http://gcn.gsfc.nasa.gov/gcn3/5548.gcn3

Spearman, C. 1904, Am J Psychol, 15, 72

Stanek, K. Z., et al. 2003, ApJ, 591, L17.

Stanek, K. Z., et al. 2007, ApJ, 654, L21

Stefanescu, A., et al. 2006, GCN, 5291, http://gcn.gsfc.nasa.gov/gcn3/5291.gcn3

Terra, F., et al. 2007, GCN, 6458, http://gcn.gsfc.nasa.gov/gcn3/6458.gcn3

Thoene, C. C., Fynbo, J. P. U., & Jakobsson, P. 2006, GCN, 5747,
http://gcn.gsfc.nasa.gov/gcn3/5747.gcn3

Thoene, C. C., Fynbo, J. P. U., & Williams, A. 2007, GCN, 6389,
http://gcn.gsfc.nasa.gov/gcn3/6389.gcn3

Thoene, C. C., Kann, D. A., Augusteijn, T., & Reyle-Laffont, C.
2007, GCN, 6154, http://gcn.gsfc.nasa.gov/gcn3/6154.gcn3

van Paradis, Kouveliotou, C., and Wijers, R.A.M 2000 ARAA, 38, 379.

Villasenor, J.S., et al. 2005, Nature, 437, 851.

Woosley, S. E., 1993, ApJ, 405, 273.

Woosley, S.E. & Bloom, J.S. 2006, ARAA, 44, 507

Wo\'zniak, P. R., Vestrand, W. T., Wren, J. A., White, R. R., Evans, S. M., & Casperson, D. 2005,
ApJ, 627, L13

Yost, S. A., et al. 2007, ApJ, 657, 925

Zhang, B., et al. 2006, ApJ, 642, 354

Zhang, B., et al. 2007, ApJ, 655, 989

Zhang, Z.-B. & Choi, C.-S. 2007, MNRAS, in press (astro-ph 0708.4049)

TABLE 1
Swift Short GRBs with X-ray or Optical Data at 11 Hours

GRB	γ-Ray[1] Fluence (10^{-7} erg/cm^2)	γ-ray[1] Fluence Error (10^{-7} erg/cm^2)	X-ray Integral Flux .3-10keV @ 11hrs (10^{-13}erg /cm^2-s)	X-ray Integral Flux Error[2] (10^{-13}erg /cm^2-s)	X-ray Spectrum Photon Index	X-ray[2] Flux @ 3 keV @ 11hrs 10^{-3} (μ Jy)	X-ray[2] Flux Error 10^{-3} (μ Jy)	R-band Mag	R-band Mag Error	R or
050509B	0.095	0.024	-	-	-	-	-	>22	-	
050724	9.98.	1.20	1.78	0.68	1.83	7.54	2.98	21.9	0.2	
050813	0.44	0.11	-	-	-	-	-	>23	-	
051210	0.85	0.14	-	-	-	-	-	-	-	
051221A	11.5	0.35	10.0	2.5	1.86	42.2	10.6	21.9	0.5	
051227	6.99	1.08	0.98	0.22	1.66	4.38	0.98	25.8	0.3	
060313	11.3	0.45	4.68	2.22	2.14	16.9	8.0	-	-	
060502B	0.40	0.05	-	-	-	-	-	>24.3	-	
060801	0.80	0.10	0.14	UL	2.03	0.52	UL	-	-	
061006	14.2	1.42	1.76	0.86	1.63	7.90	3.84	-	-	
061201	3.34	0.27	2.03	1.08	1.64	9.11	4.84	22.3	0.3	
061210	11.1	1.76	-	-	-	-	-	>23.5	-	
061217	0.42	0.07	0.66	0.42	1.36	3.00	1.90	-	-	
070714B	5.00	0.30	0.71	0.23	1.81	3.05	0.97	23.5	0.3	
070724A	0.30	0.07	1.84	1.44	2.09	6.85	5.36	-	-	
070729	1.00	0.20	0.17	0.12	2.00	0.66	0.45	-	-	

[1] BAT prompt fluence in 15-150 keV band. Data from Sakamoto et al. (2007)
[2] XRT flux at 3 keV at 11 hours after the burst trigger. Error includes 10% systematic uncertainty.
[3] Hours after burst trigger of optical data or code for optical data. If a number, it is the time after the burst (typically listed for GCN only data). If letters, the first letter is for F = full light curve, I = interpolated between measured values on either side of 11 hours, and E = extrapolated from measured data. The lower case letters indicate if the data in the referenced papers was in magnitude or Jansky units (mmf = first two references in magnitude units, third reference in Jansky units)
[4] Optical data in R-band at 11 hours after the burst trigger. R-band flux estimated from typical burst spectra if data taken in other bands. Error includes 10% systematic uncertainty.

Table References:

1. Misra & Pandey (2005)
2. Malesani et al. (2007)
3. Bikmaev et al. (2005)
4. Soderberg et al. (2006)
5. Berger & Soderberg (2005)
6. Schmidt & Bayliss (2006)
7. Price et al. (2006)
8. D'Avanzo et al. (2006)
9. Cenko, Fox & Price (2006)
10. Levan et al. (2007)

TABLE 2

Swift Long GRBs with X-ray Detections and Optical Detections or Low Upper Limits at 11 Hours

GRB	γ-Ray[1] Fluence (10^{-7} erg/cm^2)	γ-ray[1] Fluence Error (10^{-7} erg/cm^2)	X-ray Integral Flux .3-10keV @ 11hrs (10^{-13}erg /cm^2-s)	X-ray Integral Flux Error[2] (10^{-13}erg /cm^2-s)	X-ray Spectrum Photon Index	X-ray[2] Flux @ 3keV @ 11hrs 10^{-3} (μ Jy)	X-ray[2] Flux Error 10^{-3} (μ Jy)	R-band Mag	R-band Mag Error	R or
WITH OPT @ 11 hr										
050315	32.2	1.5	58.2	8.85	2.01	227.	35.	20.84	0.20	
050319	13.1	1.5	47.8	12.9	2.16	170.	46.	20.2	0.1	
050416A	3.67	0.37	15.2	2.46	2.03	58.7	9.51	21.2	0.1	
050525A	153.	2.2	22.7	4.29	1.81	97.2	18.4	19.6	0.10	
050721	36.2	3.2	23.2	4.46	1.63	104.	20.1	21.4	0.5	
050730	23.8	1.5	66.1	8.14	1.71	292.	36.	20.3	0.1	
050801	3.10	0.48	2.17	0.58	1.76	9.4	2.54	21.5	0.3	
050802	20.0	1.6	16.7	2.53	1.80	71.8	10.9	20.8	0.2	
050820A	34.4	2.4	196.	21.7	2.01	769.	85.	18.9	0.1	
050824	2.66	0.52	10.9	4.68	1.89	45.4	19.4	21.2	0.2	
050908	4.83	0.51	1.56	0.44	1.74	6.84	1.91	22.0	0.4	
050922C	16.2	0.5	8.78	1.98	2.00	34.5	7.8	20.59	0.27	
051109A	22.0	2.7	56.5	11.1	1.95	227.	45.	19.7	0.1	
051111	40.8	1.3	6.83	1.57	2.25	22.6	5.2	20.1	0.1	
060108	3.69	0.37	2.20	0.78	1.79	9.48	3.36	22.5	0.3	
060124	4.61	0.53	292.	37.5	2.13	1058.	136.	19.1	0.1	
060206	8.31	0.42	22.1	6.62	2.27	71.9	21.6	18.9	0.1	F
060210	76.6	4.1	84.8	13.0	2.06	322.5	49.3	23.6	0.1	
060418	83.3	2.5	6.15	1.56	1.77	25.7	6.8	20.2	0.1	
060512	2.32	0.40	3.47	0.98	1.61	15.6	4.4	20.66	0.16	
060526	12.6	1.7	6.74	2.40	1.84	28.5	10.2	19.7	0.1	
060604	4.02	1.06	12.9	2.87	1.80	55.4	12.3	21.16	0.19	
060605	8.89	2.35	6.07	1.26	2.38	17.9	3.7	20.7	0.2	
060607A	25.5	1.1	25.3	4.53	1.53	115.	20.6	20.4	0.3	
060714	28.3	1.7	11.3	2.96	1.73	49.7	13.0	21.01	0.16	
060729	26.1	2.1	192.	57.9	2.15	688.	207.	17.35	0.18	
060904B	16.2	1.4	7.24	1.71	2.08	27.1	6.4	21.0	0.2	
061007	444.	10.0	13.3	1.34	1.84	56.3	5.66	21.0	0.2	
061021	29.6	1.0	45.3	5.65	1.83	193.	24.	20.06	0.09	
061110A	10.6	0.8	0.96	0.39	1.56	4.34	1.75	22.85	0.27	
061121	137.	2.0	96.6	13.5	1.70	428.	60.	20.1	0.1	
061126	67.7	2.2	41.9	4.98	1.69	186.	22.	21.4	0.1	
070224	3.05	0.51	3.04	1.72	1.64	13.6	7.7	22.96	0.27	
070419B	75.0	2.0	106.	15.9	1.67	474.	71.	22.6	0.2	
070508	200.	3.0	44.0	4.77	1.79	190.	21.	22.6	0.2	
070518	1.60	0.20	1.47	0.33	1.92	6.01	1.36	22.5	0.2	
OPTICAL LIMIT @ 11 hr										
050713B	31.8	3.2	102.	22.3	1.87	427.	93.	>23.2	-	
061004	5.66	0.31	2.53	1.20	1.99	9.96	4.74	>22.0	-	
061222A	83.4	1.6	262.	36.3	2.06	900.	138.	>23.8	-	
070621	43.0	1.0	11.5	2.46	2.08	43.0	9.2	>23.4	-	
070704	59.0	3.0	6.22	3.65	1.76	27.1	15.9	>23.0	-	
070721A	0.71	0.18	2.42	1.03	2.48	6.48	2.75	>24.0	-	1

[1] BAT prompt fluence in 15-150 keV band. Data from Sakamoto et al. (2007)
[2] X-ray flux at 3 keV at 11 hours after the burst trigger. Error includes 10% systematic uncertainty.
[3] Hours after burst trigger of optical data or code for optical data. If a number, it is the time after the burst (typically listed for GCN only data). If letters, the first letter is for F = full light curve, I = interpolated between measured values on either side of 11 hours, and E = extrapolated from measured data. The lower case letters indicate if the data in the referenced papers was in magnitude or Jansky units (mmf = first two references in magnitude units, third reference in Jansky units)
[4] Optical data in R-band at 11 hours after the burst trigger. R-band flux estimated from typical burst spectra if data taken in other bands. Error includes 10% systematic uncertainty.

Table References:

1. Cobb & Bailyn (2005)
2. Wozniak et al. (2005)
3. George et al. (2006)
4. Huang et al. (2007)
5. Kamble, Resmi, & Misra (2007)
6. Ghirlanda, Nava, Ghisellini, & Firmani (2007)
7. Soderberg et al. (2007)
8. Shao & Dai (2005)
9. Della Valle et al. (2006)
10. Antonelli et al. (2006)
11. Pandey et al. (2006)
12. Chen et al. (2007)
13. Rykoff et al. (2006)
14. Cenko et al. (2006)
15. Sollerman et al. (2007)
16. Durig \& Price (2005)
17. Yost et al. (2007)
18. Butler et al. (2006)
19. Guidorzi et al. (2007a)
20. Oates et al. (2006)
21. Misra et al. (2007)
22. Monfardini et al. (2006)
23. Stanek et al. (2007)
24. Curran et al. (2007a)
25. Dado, Dar & De Rujula (2007)
26. Curran et al. (2007b)
27. Hicken & Garnavich (2006)
28. Milne (2006)
29. Dai et al. (2007)
30. Garnavich & Karska (2006)
31. Nysewander et al. (2007)
32. Melandri, Tanvir & Guidorzi (2006)
33. Quimby & Rykoff (2006)
34. Soyano, Mito, & Urata (2006)
35. Mundell et al. (2007)
36. Thoene, Fynbo & Jakobsson (2006)
37. Fynbo (2006)
38. Page et al. (2007)
39. Perley et al. (2007)
40. Thoene et al. (2007)
41. Schmidt \& Mackie (2007)
42. Thoene, Fynbo, & Williams (2007)
43. Terra et al. (2007)

44. Sharapov, D. et al. (2005)
45. Berger, E. et al. (2006)
46. Efimov, Yu. et al. (2006)
47. Malesani, D., et al. (2007)
48. Melandri, A., et al. (2007)
49. Malensani, E., et al. (2007)

TABLE 3

Swift Long GRBs with X-ray Detections but No Optical Data at 11 Hours

GRB	γ-Ray[1] Fluence (10^{-7} erg/cm^2)	γ-ray[1] Fluence Error (10^{-7} erg/cm^2)	X-ray Integral Flux .3-10keV @ 11hrs (10^{-13} erg /cm^2-s)	X-ray Integral Flux Error[2] (10^{-13} erg /cm^2-s)	X-ray Spectrum Photon Index	X-ray Flux @ 3keV @ 11hrs 10^{-3} (μ Jy)	X-ray[2] Flux Error 10^{-3} (μ Jy)
050124	11.9	0.7	14.7	4.96	2.02	57.3	19.3
050128	50.2	2.3	44.9	6.58	1.99	178.	26.0
050215B	2.27	0.29	3.02	2.03	1.62	13.6	9.12
05219B	158.	5.	49.2	6.50	2.02	191.6	25.3
050223	6.36	0.65	1.20	0.86	2.16	4.25	3.05
050326	88.6	1.5	28.8	9.67	1.81	123.	41.4
050505	24.9	1.8	34.2	4.95	2.02	132.6	19.2
050603	63.6	2.3	28.9	4.77	1.76	125.7	20.8
050607	5.92	0.55	2.22	0.67	2.17	7.83	2.36
050712	10.8	1.2	12.5	2.20	2.10	46.4	8.15
050713A	51.1	2.1	35.4	6.29	2.06	134.7	23.9
050714B	5.95	1.05	5.48	3.61	2.22	18.7	12.3
050716	61.7	2.4	7.94	0.92	1.26	35.9	4.15
050726	19.4	2.1	5.76	1.50	2.16	20.5	5.34
050814	18.6	2.1	12.1	2.58	2.08	45.5	9.69
050819	3.50	0.55	2.73	1.30	1.82	11.6	5.56
050822	24.6	1.7	23.3	3.64	1.94	94.6	14.8
050826	4.13	0.72	5.38	1.75	1.76	23.4	7.63
050911	3.17	0.58	1.54	0.6	2.33	4.78	1.9
050915A	8.50	0.88	4.31	1.57	1.92	17.6	6.45
050915B	35.1	1.1	7.94	4.78	2.06	30.1	18.1
051001	17.4	1.5	3.27	1.09	2.00	12.8	4.27
051008	50.6	1.5	14.6	2.98	1.86	61.3	12.5
051016B	1.70	0.22	13.9	5.0	1.86	58.5	21.
051117A	43.4	1.5	6.98	0.82	1.98	27.8	3.25
060105	176.	10.0	34.4	15.	2.11	126.7	55.
060109	6.55	1.03	9.94	3.10	2.40	28.8	9.00
060115	17.1	1.5	9.70	6.44	2.26	31.82	21.1
060202	21.3	1.6	41.9	7.15	2.32	131.4	22.4
060204B	29.5	1.8	11.0	2.34	2.07	41.4	8.82
060211A	15.7	1.4	4.87	1.86	2.23	16.4	6.29
060218	3.74	0.77	42.3	13.8	3.71	19.4	6.33
060219	4.28	0.80	1.41	0.53	1.86	5.91	2.23
060306	21.3	1.2	21.8	4.22	2.19	75.5	14.6
060319	2.64	0.34	13.2	2.70	1.87	55.2	11.3
060428A	13.9	0.8	103.	40.	2.07	389.	151.
060428B	8.23	0.81	3.37	0.65	1.81	14.4	2.78
060507	44.5	2.3	10.4	2.63	2.00	41.1	10.4
060510A	80.5	3.1	300.	46.7	1.81	1281.	200.
060510B	40.7	1.8	1.64	0.66	2.09	6.14	2.48
060512	2.32	0.40	3.47	0.98	1.61	15.65	4.39
060707	16.0	1.5	18.0	5.01	1.65	80.5	22.4
060708	4.94	0.37	8.16	1.41	1.92	33.4	5.75
060712	12.4	2.2	4.21	1.12	2.23	14.2	3.76
060804	5.98	0.99	18.2	7.62	2.20	62.9	26.4
060807	8.48	1.09	14.9	2.72	2.26	49.0	8.92
060813	54.6	1.4	55.3	6.48	1.80	237.	27.8
060814	145.	2.	59.9	9.11	2.29	192.	29.2
060923A	8.69	1.33	5.49	1.29	2.00	21.6	5.06
060923C	15.8	2.2	7.01	2.43	2.52	18.0	6.23
061019	25.9	4.1	19.1	8.71	1.60	86.3	39.4
061110A	10.6	0.8	0.96	0.39	1.56	4.34	1.75
070103	3.38	0.46	1.18	0.39	1.87	4.92	1.64
070107	51.9	2.6	50.0	8.54	2.23	169.	28.9

070129	30.7	2.7	22.2	6.62	2.11	81.5	24.3
070208	4.47	1.0	5.36	2.29	1.83	22.8	9.72
070220	106.	2.3	8.10	2.55	1.60	36.6	11.5
070306	55.0	3.0	143.	37.0	2.19	496.	128.
070318	23.0	1.0	19.8	2.47	1.22	89.2	11.1
070328	89.0	2.0	54.7	8.41	1.79	236.	36.3
070330	1.80	0.30	4.55	1.12	2.19	15.7	3.88
070412	4.80	0.70	4.00	1.71	2.00	15.7	6.71
070419B	75.0	2.0	106.	15.9	1.67	473.7	70.8
070420	140.	4.	69.1	10.7	1.90	285.3	44.1
070508	200.	4.	44.0	4.77	1.79	189.7	20.5
070518	1.60	0.20	1.47	0.33	1.92	6.01	1.36
070521	80.0	2.0	29.6	5.37	1.72	131.	23.7
070529	26.0	2.0	5.02	1.36	1.81	21.5	5.83
070611	3.90	0.60	2.33	0.76	1.71	10.3	3.35
070616	192.	3.	9.76	2.74	2.34	30.1	8.45
070721B	35.0	2.0	4.79	1.62	1.74	21.0	7.08

[1] BAT prompt fluence in 15-150 keV band. Data from Sakamoto et al. (2007)
[2] XRT flux at 3 keV at 11 hours after the burst trigger. Error includes 10% systematic uncertainty.

TABLE 4
Correlation Fits and Coefficients

Data Set	Number of Data Points N	a[1]	b[1]	Correlation Coefficient r	Null[2] Hypothesis Probability P_{null}	Fraction of variability due to correlation r^2
Optical (Y) *vs* X-ray (X) Long GRBs	36	1.50±0.01	0.22±0.01	0.25	0.13	0.06
Optical (Y) *vs* X-ray (Y) Short GRBs	5	1.80±0.48	0.60±0.22	0.35	0.43	0.12
X-ray (Y) *vs* Gamma-ray (X) Long GRBs	113	1.23±0.07	0.41±0.01	0.43	$4x10^{-6}$	0.18
X-ray (Y) *vs* Gamma-ray (X) Short GRBs	10	2.23±0.60	0.70±0.10	0.63	0.05	0.40
Fluence (Y) *vs* Peak Flux (X) Long GRBs	175	-5.98±0.01	0.77±0.02	0.70	$2x10^{-20}$	0.49
Fluence (Y) *vs* Peak Flux (X) Short GRBs	17	-7.30±0.03	1.00±0.10	0.51	0.04	0.26

[1] Fit with function $Y = 10^a X^b$

[2] The significance of the correlation is $1 - P_{null}$

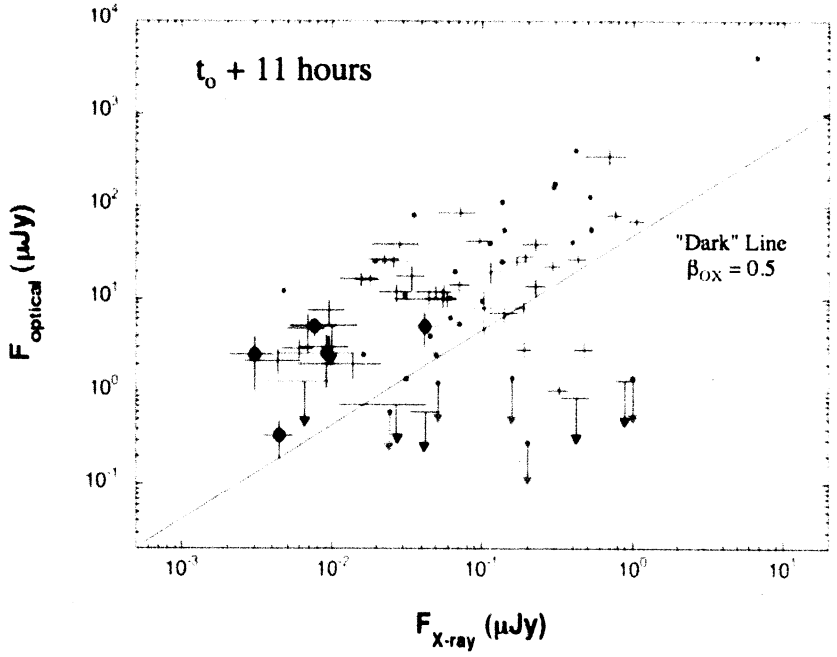

Figure 1:

The X-ray afterglow *vs* optical afterglow fluxes of *Swift* short and long GRBs at 11 hours after the burst. The crosses and black filled circles are *Swift* long and short bursts, respectively, and the small gray circles are the pre-*Swift* GRBs taken from Jakobsson et al (2004). The XRT X-ray fluxes are at 3 keV and the optical fluxes are in the R-band (see Table 1 and 2). Also shown is the 'dark' burst separation line in the Jakobsson et al paper (2004).

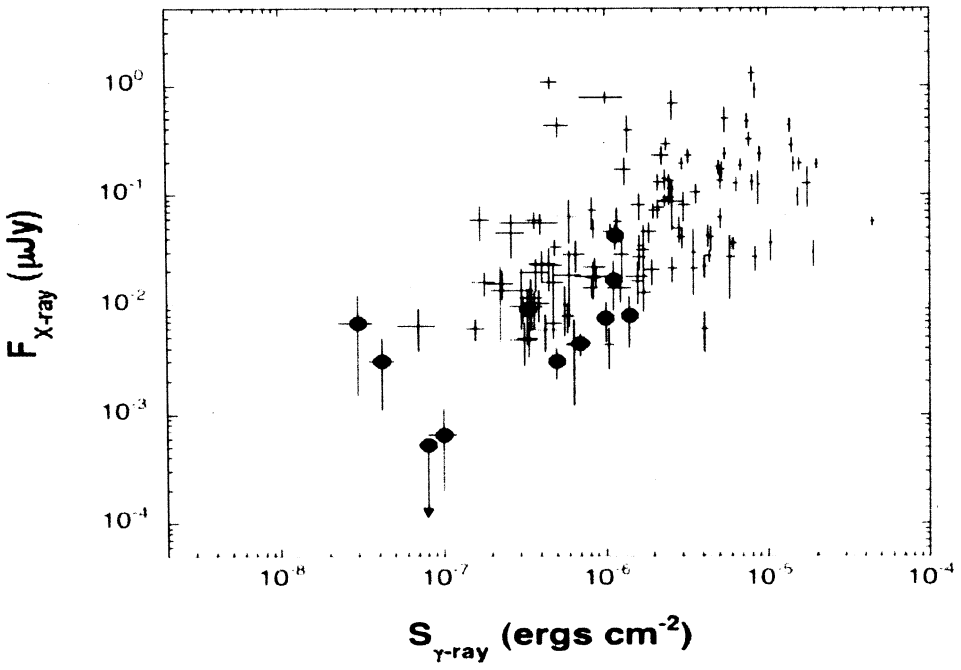

Figure 2:

The X-ray afterglow flux *vs* gamma-ray prompt fluence of *Swift* short and long GRBs at 11 hours after the burst. The crosses are *Swift* long bursts and the black filled circles are *Swift* short bursts. The XRT X-ray fluxes are at 3 keV and the BAT gamma-ray fluences are between 15 and 150 keV. The XRT and BAT data are given in Table 1, 2 and 3. The BAT data are from Sakamoto et al. (2007).

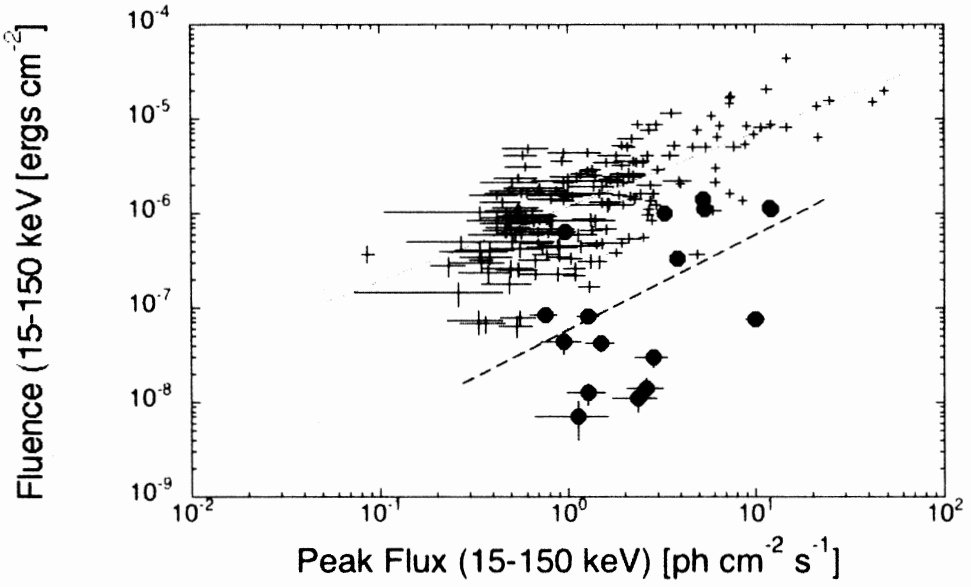

Figure 3:

The prompt gamma-ray fluence *vs* peak flux measured by BAT in the 15 to 150 keV band for all bursts through February 2007. Short bursts are shown by filled circles and long bursts by crosses. The dotted line is the best fit to the *Swift* long burst data and the dashed line to the short burst data (see Table 4). The data are from Sakamoto et al. (2007).